Holographic Optical Fibre Switching with High Isolation

Haozhi Wang
School of Electronic and Science and Engineering
Southeast University
Nanjing,China
whz@seu.edu.cn

Jiewen Nie
School of Electronic and Science and Engineering
Southeast University
Nanjing,China
jwnie@seu.edu.cn

Ruixue Guo
School of Electronic and Science and Engineering
Southeast University
Nanjing,China
guo_rx@seu.edu.cn

Haining Yang
School of Electronic and Science and Engineering
Southeast University
Nanjing,China
h.yang@seu.edu.cn

***Abstract*—This work demonstrates a neural-network-enabled holographic optical switch with a worst-case and median isolation of >26dB and >48dB across the 0-15dB attenuation range, which is >6dB improvement over the state of art.**

Keywords— WSS, Neural-network, Holographic

I. INTRODUCTION

Wavelength selective switch (WSS) [1-2] based on liquid on silicon (LCOS) devices have been widely used in the modern telecommunication networks and datacentre interconnecting networks. A typical WSS is able to route the optical signals from the common input port to any of the output ports by reconfiguring the beam steering holograms displayed on the LCOS device. The power difference between the target port and the untargeted ports is referred to as the port isolation. In the ROADM [3] networks where the WSSs are also used for spectrum equalisation, the beam steering holograms must be able to attenuate the optical signal into the target port. In this case, the crosstalk levels at the untargeted ports need further suppression to maintain the port isolation. This is extremely challenging and requiring sophisticated design of the beam-steering holograms, especially for high (>20) port count switches.

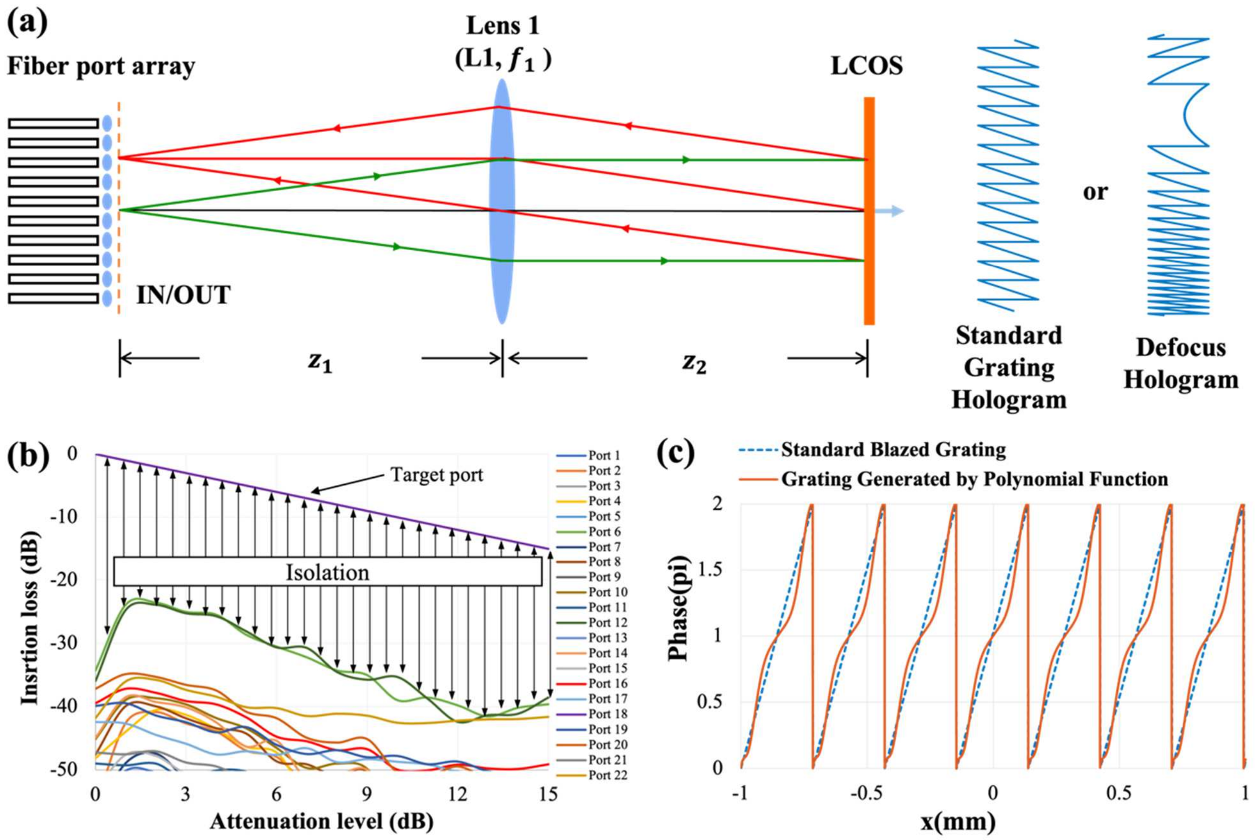

Fig.1 (a) General architecture of a holographic optical switch; (b) typical port isolation performance across the attenuation range; (c) Phase profiles of the standard blaze gratings and polynomial gratings used in this paper.

Natural Science Foundation of China (6506009768 and 6506009778);
Natural Science Foundation of Jiangsu Province (BK20200351).

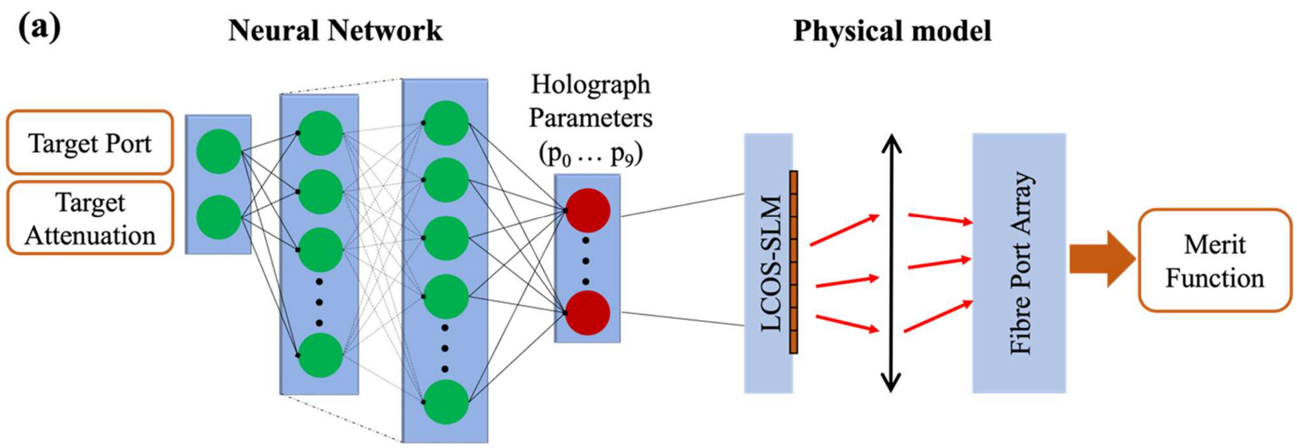

Fig.2 Architecture of the end-to-end neural networks for the parameterised hologram generation.

In this work, we constructed an end-to-end neural network that incorporated a physical model of the holographic optical switch. The neural network was able to generate a series of polynomial coefficients that were used to describe the desired beam steering holograms in a parameterised fashion. The performance of this neural network was validated in a 1×22 holographic optical switch, achieving worst-case and median isolation of >26 dB and >48 dB, respectively, across the 0~15dB attenuation range.

II. System And Methods

Fig. 1(a) shows the core 2f switching optical architecture of a typical 1×N WSS. This also illustrated the experimental setup used in this work. At the IN/OUT plane, a 1×23 linear fibre array has a pitch of 250 µm (1 input and 22 output). The main switching lens had a focal length(f_1) of 150 mm. The phase-only LCOS device used in this work had a resolution of 1920×1200 with a pixel size of 8 µm. Its total phase depth was 2.5**π** at 1550 nm.

In the standard setup, the collimated fibre array was placed at the front focal plane of the main switching lens and the LCOS device was placed at the back focal plane of L1. In this case, the input beam has a waist of ~1.05 mm, covering <400 pixels of the LCOS device. Blazed gratings with variable periods were used to realise the beam steering. When the attenuation was required, additional sinusoid or square features [4] are added on top of the blazed gratings to reduce the diffraction efficiency of the +1st order as well as suppress the higher orders. Since all the diffraction orders were focused at the IN/OUT plane, they are likely to be coupled into the fibre ports with high efficiency. As a result, it is challenging to maintain a good isolation. Fig. 1(b) showed a typical port isolation performance for a specific output port across the 0-15 dB attenuation range. It can be seen that the worst-case port isolation occurred at 1.5 dB attenuation.

In order to address this issue, our previous works [5-6] introduced an intentional defocus into the optical system by moving the collimated fibre array or the LCOS device away from the focal plane of the main switching lens. In this work, we moved the collimated fibre array closer to the main switching lens. The value of z1 was set as 85 mm. In this case, the LCOS device needs to display Fresnel lens phase holograms to compensate for the defocus for the +1st diffraction order only. While the +1st diffraction order would still be coupled into the target port with high efficiency, higher diffraction orders will be defocused at the IN/OUT plane, spreading over multiple output ports with low coupling efficiency. As the result, the worst-case isolation can be significantly improved. However, ports that were not affected by higher diffraction order in the standard setup are also likely to suffer from a moderate level of crosstalk. In other words, the median isolation level is sacrificed for improving the worst-case isolation in this defocused setup.

In this work, we aimed to achieve simultaneously high worst-case and median isolation level in a standard optical setup without any defocus by using a customised end-to-end neural network. In order to realise a high training efficiency, the beam steering holograms were parameterised. As shown in Fig. 1(c), the phase profile of individual grating period was described by a series of polynomial coefficients (pi). In this case, the neural network is only required to generate a limited number of polynomial coefficients instead of the phase level of each pixel within the beam steering holograms. The end-to-end neural network shown in Fig. 2 was constructed and trained to generate the optimal hologram parameter (pi) set for any target port at any attenuation level. The neural network contained six fully connected layers for fitting the best performance functions in the parameters space. During the training process, the network incorporated a differentiable physical model of the optical switch based on the Fresnel diffraction theory. The phyiscal model was used to evaluate performance the beam steering holograms based on the predicted insertion loss level and port isolation values until the network converges. A well-trained neural network can generate the optimal polynomial coefficients for the holograms to achieve an arbitrary attenuation levels for any target ports, while maintaining the highest possible port isolation.

III. Experimental Results

The performance of the three setups described in the above were experimentally validated in this work for all the target port and attenuation level configurations. The range of attenuation is between 0 dB and 15 dB, which reflected typical scenarios used in a ROADM network. Fig. 3(a) shows the results for the standard setup without any defocus. The worst-case isolation was as low as <20 dB for certain switching configurations. This would introduce unacceptable level of noises into the ROADM networks. As shown in Fig. 3(b), the introduction of the defocus led to >6 dB improvement in the

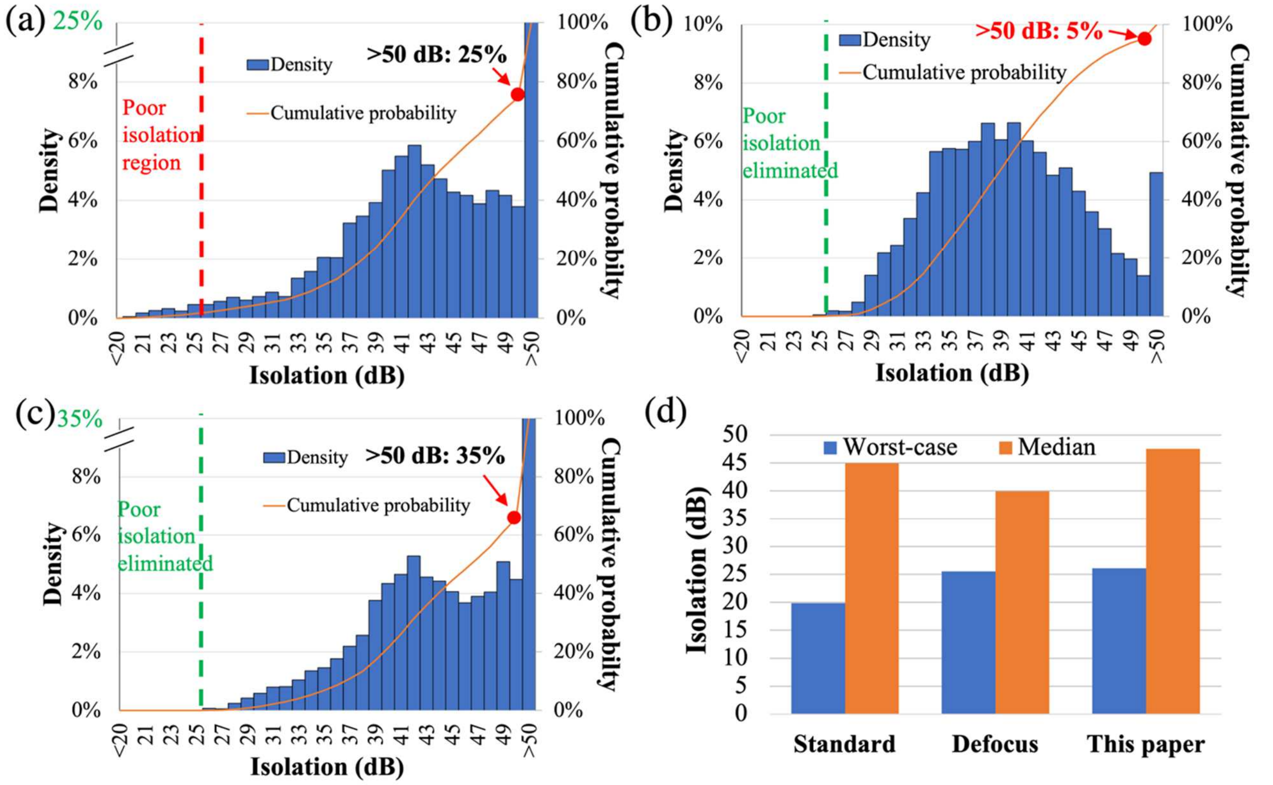

Fig.3 Isolation distribution for all the switching configurations: (a) standard setup, (b) defocused setup, and (c) this paper. (d) The worst-case and median isolation in standard setup, defocused setup and this paper.

worst-case isolation. Switching configurations with an isolation level <25 dB were completely eliminated in this case. However, the untargeted ports were more likely to be impacted by a moderate level of crosstalk. For example, the median isolation level was reduced from 45dB to 40dB. In addition, the probability of a port with an isolation >50 dB was also reduced from 25% to only 5%. This is consistent with our theoretical analysis that the introduction of defocus would spread the crosstalk from a single port to multiple ports. Fig. 3(c) shows the experiment results in a standard system without any defocus but using the beam steering holograms generated by our neural networks. Our method managed to further increase the worst-case isolation to ~26 dB, which is even better than the results obtained in the defocused setup. More importantly, the median isolation level was also improved to ~48 dB and the probability of a port with an isolation >50 dB was increased to 35%. It is a significant improvement over the state-of-art and would enhance the transmission performance of a ROADM networks.

IV. Conclusion

This work demonstrated a holographic optical switching with high isolation. This was enabled by a customised neural network that incorporated the physical model of the optical system and the parameterised beam steering holograms. The experimental results achieved worst-case and median isolation of >26 dB and >48 dB, respectively, across the whole 0~15 dB attenuation range. Both are 6 dB higher than the state-of-art.

Acknowledgment

This work has been supported by Natural Science Foundation of China (6506009768 and 6506009778); Natural Science Foundation of Jiangsu Province (BK20200351).

References

[1] G. Baxter et al., "Highly programmable wavelength selective switch based on liquid crystal on silicon switching elements," in Optical Fiber Communication Conference, 2006.

[2] H. Yang et al., "24 [1×12] Wavelength Selective Switches Integrated on a Single 4k LCoS Device," JLT, vol. 39, no. 4, pp. 1033–1039, 2021

[3] P. D. Colbourne and B. Collings, "ROADM switching technologies," in Optical Fiber Communication Conference, 2011.

[4] M. Nakajima et al., "Analysis and suppression of high-order diffractions in liquid-crystal-based spatial light modulator for photonic switch application," Japanese J. of Applied Physics, vol. 56, no. 9, 2017.

[5] B. Robertson et al., "Reduction of crosstalk in a colourless multicasting LCOS-based wavelength selective switch by the application of wavefront encoding," in Proceedings of SPIE, vol. 8284, p. 82840S, 2012

[6] B. Robertson et al., "Application of the Fractional Fourier Transform to the Design of LCOS Based Optical Interconnects and Fiber Switches," Applied Optics, vol. 51, no. 12, pp. 2212–2222, 2012.